# Biomass and leaf-area index maps derived from SPOT images for Toolik Lake and Imnavait Creek areas, Alaska

**Margaret M. Shippert, Donald A. Walker, Nancy A. Auerbach, and Brad E. Lewis**

Institute for Arctic and Alpine Research, Campus Box 450, University of Colorado, Boulder, Colorado 80309-0450, USA

*Received July 1994*

ABSTRACT. A new emphasis on understanding natural systems at large spatial scales has led to an interest in deriving ecological variables from satellite reflectance images. The normalized difference vegetation index (NDVI) is a measure of canopy greenness that can be derived from reflectances at near-infrared and red wavelengths. For this study we investigated the relationships between NDVI and leaf-area index (LAI), intercepted photosynthetically active radiation (IPAR), and biomass in an Arctic tundra ecosystem. Reflectance spectra from a portable field spectrometer, LAI, IPAR, and biomass data were collected for 180 vegetation samples near Toolik Lake and Imnavait Creek, Alaska, during July and August 1993. NDVI values were calculated from red and near-infrared reflectances of the field spectrometer spectra. Strong linear relationships are seen between mean NDVI for major vegetation categories and mean LAI and biomass. The relationship between mean NDVI and mean IPAR for these categories is not significant. Average NDVI values for major vegetation categories calculated from a SPOT image of the study area were found to be highly linearly correlated to average field NDVI measurements for the same categories. This indicates that in this case it is appropriate to apply equations derived for field-based NDVI measurements to NDVI images. Using the regression equations for those relationships, biomass and LAI images were calculated from the SPOT NDVI image. The resulting images show expected trends in LAI and biomass across the landscape.

**Contents**



## Introduction

### Advantages of remotely sensed observations of ecological variables

The new emphasis in the natural sciences on the understanding of global scale phenomena has prompted ecologists to seek methods by which ecological data can be collected at large spatial scales. For example, calculating fluxes of trace gases from a region would require estimates of the spatial extent and variability across the region of ecological variables that control these fluxes. Collection of such data through field surveys is usually not feasible because of financial and time limitations. Remotely sensed reflectance data provide an alternative means for making these estimates.

Additional advantages of remotely sensed reflectance data include the non-destructive nature of reflectance measurements. Moreover, they record the actual rather than the potential state of ecological variables, because they include any local perturbations. For example, effects of variation in soils, topography, vegetation history, disturbance regimes, or anthropogenic perturbations (such as agriculture and development) are inherent in remotely sensed data (Box and others 1989; Prince 1991; Walker and Walker 1991). Commonly used bioclimatic estimates of ecological variables, on the other hand, can only describe the vegetation that is expected on the basis of average climatic conditions.

### Objective of this study

The objective of this study was to investigate the feasibility of deriving variables of ecological interest from satellite multispectral reflectance images of Arctic tundra. A particular interest in studying aspects of the carbon cycle led to examining the relationships between reflectance and biomass, leaf-area index (LAI), and intercepted photosynthetically active radiation (IPAR), because these ecological variables are relevant to this cycle. LAI is a measure of the density of foliage. IPAR is an indication of the photosynthetic rate of the canopy. Biomass is a measure of the amount of carbon stored in the canopy. Many previous studies have examined relationships between reflectance and biomass, LAI, and IPAR in temperate ecosystems and crops (for example, Biscoe and others 1975; Hodges and Kanemasu 1977; Asrar and others 1985). LAI and IPAR have been used in crop yield and evapotranspiration models and vegetation monitoring efforts (for example, Wiegand and others 1979; Steven and others 1983; Hatfield and others 1984).

### Vegetation indices

When sunlight falls on green vegetation, red wavelengths (near 0.6 $\mu$m) are absorbed by chloroplasts, while near-infrared wavelengths (0.7–0.9 $\mu$m) are reflected. Because this spectrum is unique to vegetation, one way to infer the amount of vegetation existing in a pixel of a multispectral reflectance image is to compare the reflectance for that pixel at red wavelengths to the reflectance at near-infrared wavelengths. If the near-infrared reflectance is much larger than the red reflectance, then presumably there is a considerable amount of green vegetation present. The use of a ratio of near-infrared to red light for estimating vegetation amount was first reported by Jordan (1969). He used a ratio of light transmitted to the forest floor at 0.800 and 0.675 $\mu$m to derive the leaf-area index for forest

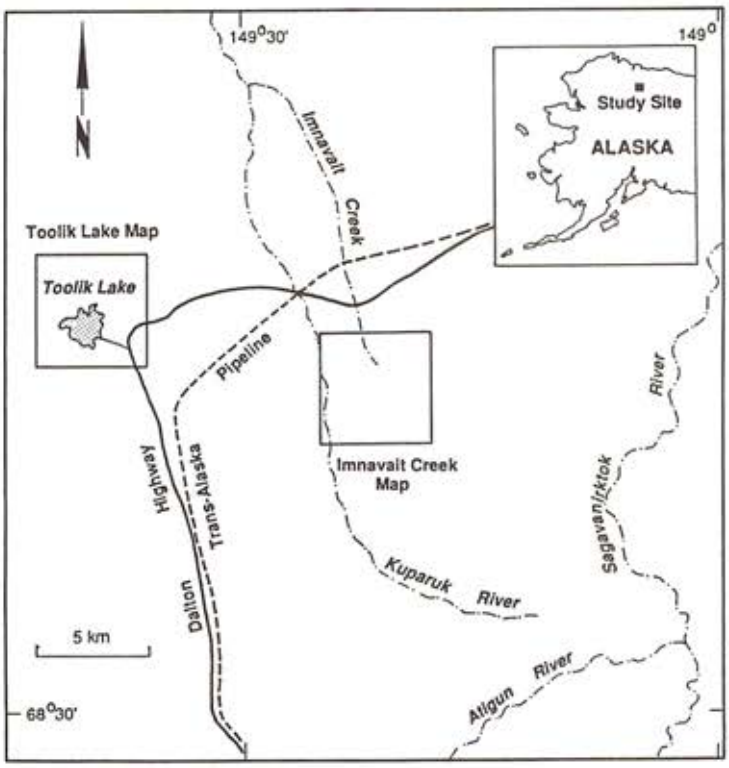


Fig. 1. The study site.

canopies in a tropical rain forest. Studies by Colwell (1973, 1974) concluded that the ratio of reflected infrared light to reflected red light was useful for estimating biomass of a grass canopy. This ratio is referred to today as the simple vegetation index or simple ratio. Rouse and others (1973, 1974) developed what we now refer to as the normalized difference vegetation index (NDVI), which is the difference between near-infrared and red reflectances divided by their sum. Many other variations of the vegetation index have been developed over the years. In general, however, the different vegetation indices contain the same information, and are therefore considered to be functionally equivalent (Perry and Lautenschlager 1984; Tucker and Sellers 1986).

Theory suggests that vegetation index values should be proportional to IPAR (Sellers 1985, 1987, 1992; Baret and Guyot 1991). Near-infrared reflectance is proportional to twice the pathlength of solar radiation, because it travels both into and out of the canopy. IPAR is proportional to one pathlength of the radiation, because it does not travel out of the canopy. Near-infrared reflectance, therefore, should be proportional to IPAR. Consequently, if the background to the vegetation canopy is very dark, IPAR should be proportional to vegetation index values. Because IPAR is proportional to LAI (a more dense canopy results in more intercepted light), LAI should also be proportional to vegetation index values. Because, LAI is also related to biomass (the more biomass, the more dense the canopy), biomass should also be proportional to vegetation index values.

Countless studies in many different ecosystems have used some form of vegetation index to study spatial or temporal vegetation changes. Within the Arctic, Stow and others (1993) demonstrated that mean NDVI values for major vegetation types near Toolik Lake, Alaska were significantly different from each other. Walker and others (1995) have related NDVI to landscape age and other site factors in the same region. Hansen (1991); Auerbach (1992); and Hope and others (1993) have investigated the relationship between NDVI and biomass in Arctic vegetation with mixed results. The relationship between NDVI and LAI or IPAR in Arctic tundra has not been investigated before this study.

## Methods

### Study site

The study area was in the Kuparuk River watershed in the northern foothills of the Brooks Range, Alaska (Fig. 1). It included Toolik Lake, which is the site of a research station operated by the Institute for Arctic Biology at the University of Alaska, Fairbanks. This area is the focus of other Arctic ecological research programs, such as the Arctic Long-Term Ecological Research (LTER) project, the Response, Resistance, Resilience to and Recovery from Disturbance in Arctic Ecosystems (R4D) project sponsored by the US Department of Energy, and the Land–Atmosphere–Ice Interactions (LAII) flux study sponsored by the US National Science Foundation. The vegetation includes moist tussock tundra, riparian shrublands, wet sedge meadows, and dry upland heath communities. It is broadly representative of the Southern Arctic Foothills physiographic province of the North Slope of Alaska (Walker and others 1989).

### Field measurements

Reflectance spectra from a portable field spectrometer, LAI, IPAR, and above-ground biomass measurements were collected for 60 plots near Toolik Lake and Imnavait Creek, Alaska (Fig. 1) between 25 July and 10 August 1993. Plots were selected to represent a wide variety of vegetation types typical of the Southern Arctic Foothills physiognomic province. Three replicates were sampled at each plot, for a total of 180 samples. While all variables were collected at most plots, biomass was not collected at plots with tall shrubs, due to difficulties associated with clipping these plots. Reflectance spectra were collected using a PS-II portable field spectrometer manufactured by Analytical Spectral Devices, Inc. The PS-II contains a 100 mm focal length, holographic grating spectrometer designed to collect light from an external source through a bundle of 19 optical fibers. The captured light travels through the fibers and strikes a grating that diffracts the light into its component wavelengths. The diffracted light falls on the surface of a silicon photo diode array detector (Analytical Spectral Devices, personal communication).

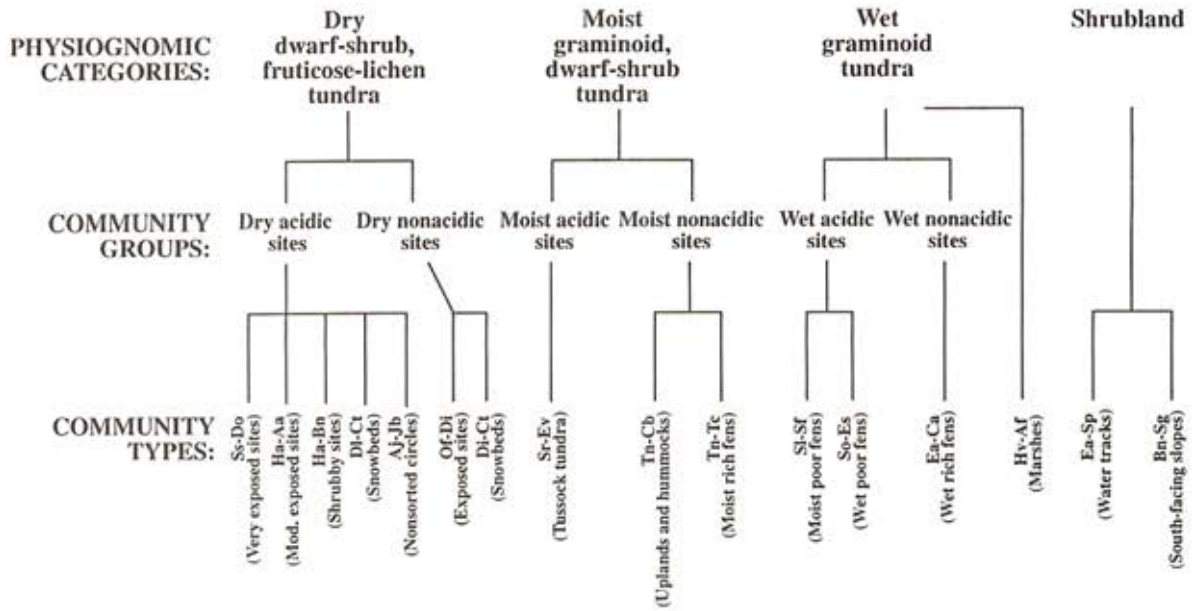


Fig. 2. The hierarchy of vegetation groupings used to combine field data. Community groups are used in Figure 6 and in Walker and others (1995). Community types are indicated by abbreviations: Aj-Jb = Anthelia juratz*kana-Juncus biglumis*; Bn-Sg = *Betula nana-Salix glauca*; Di-Ct = *Dryas integrifolia-Cassiope tetragona*; Dl-Ct = *Diapensia lapponica-Cassiope tetragona*; Ea-Ca = *Eriophorum angustifolium-Carex aquatilis*; Ea-Sp = *Eriophorum angustifolium-Salix planifolia*; Ha-Aa = *Hierochloë alpina-Arctous alpina*; Ha-Bn = *Hierochloë alpina-Betula nana*; Hv-Af = *Hippuris vulgaris-Arctophila fulva*; Of-Di = *Ochrolechia frigida-Dryas integrifolia*; Sl-Sf = *Sphagnum lenense-Salix fuscescens;* So-Es = *Sphagnum orientale-Eriophorum scheuchzeri*; Sr-Ev = *Sphagnum rubellum-Eriophorum vaginatum*; Ss-Do = *Selaginella sibirica-Dryas octopetala*; Tn-Cb = *Tomenthypnum nitens-Carex bigelowii*; and Tn-Tc = *Tomenthypnum nitens - Trichophorum caespitosum* .

The spectrometer gun was mounted on a 1-m long tripod arm, which was leveled prior to collecting measurements at each replicate plot. The effects of electron charge build-up in the silicon diode detector array of the spectrometer were removed by subtracting a spectrum collected with the shutter closed from every reflectance measurement. Atmospheric effects were removed by calibrating the spectrometer to a spectralon panel immediately prior to every reflectance measurement. NDVI values were calculated from reflectances at wavelengths corresponding to the Landsat TM red band (630–690 nm) and the near-infrared band (760–900 nm), according to equation 1:

$$NDVI = \frac{NIR - red}{NIR + red} \quad [1]$$

where NIR is the reflectance of the plot at the near-infrared band, and red is the reflectance of the plot at the red band. The spectrometer software includes an algorithm for approximating reflectance values of Landsat Thematic Mapper (TM) bands. The bandpasses for each of the TM bands is approximated by a square bandpass. The width of the square bandpass used is equal to the width at half the maximum of the corresponding TM bandpass. The reflectance value calculated for this TM band is the average PS-II reflectance within the band. Gallo and others (1987) demonstrated that NDVI calculated from TM bands is virtually identical to NDVI calculated from the French Système Probatoire d'Observation de la Terre (SPOT) bands (red: 610–680 nm; near-infrared: 790–890 nm). Therefore, the authors thought it unnecessary to develop an algorithm to approximate SPOT bands from the spectrometer data, even though working with a SPOT image for this study.

LAI was measured with a PCA-2000 plant canopy analyzer manufactured by LI-COR, Inc. IPAR was measured with a LI-1000 line quantum sensor, also manufactured by LI-COR, Inc. Total biomass was measured by collecting all above-ground organic material at each sample site within a 50 x 20 cm wire frame centered over the site of reflectance, LAI, and IPAR measurements. These biomass samples were then sorted into green, dead, and woody fractions.

**Image processing**

NDVI was also calculated from a SPOT multispectral satellite image of the study area acquired on 29 July 1989. Prior to calculation of NDVI, this image was radiometrically calibrated using coefficients provided by SPOT Image Corporation. Next, the spectrum of the darkest pixel in the image was subtracted from every other pixel spectrum to correct for atmospheric effects. Two areas in the SPOT scene, corresponding to the areas of a 1:5000 scale geobotanical map of the Toolik Lake area and a 1:6000 scale geobotanical map of the Imnavait Creek area (Walker and others 1989) (Fig. 1), were separated into different physiognomic vegetation categories using boundaries from these maps. Mean and standard deviation of NDVI values from the SPOT image for the different physiognomic vegetation categories were calculated.

## Analysis

NDVI, LAI, IPAR, and biomass data from the 180 samples were grouped into four broad physiognomic vegetation categories, and means and standard deviations of each category were calculated. The data were also grouped into 16 community types (each physiognomic category comprised several community types) (Fig. 2), and the means and standard deviations of each variable for each community type were calculated. All analyses were performed three times: once with average values for the broad physiognomic categories, once with average values for the more specific community types, and once with ungrouped data. Mean LAI, IPAR, and biomass values were plotted against the corresponding NDVI values for each data grouping. Curves were fitted to these data. Although vegetation indices are usually considered to be a function of vegetation amount, these scatterplots were constructed with NDVI as the independent variable, in order to calculate LAI, IPAR, and biomass from NDVI.

Mean and standard deviation of NDVI values from the SPOT image were compared to mean field NDVI values for the four broad physiognomic categories using linear regression. This was done in order to determine the appropriateness of applying results of analyses performed with the field measurements to the SPOT image.

Biomass and LAI images were calculated from the SPOT NDVI image. The equation from the regression of field NDVI versus SPOT NDVI was first used to convert the SPOT NDVI values to field NDVI values. LAI and biomass values were then calculated for each pixel in the image using the equation from the linear regression of NDVI versus LAI and NDVI versus biomass for physiognomic categories.

## Results

For all of the following analyses it was found that total above-ground biomass is better correlated to NDVI than green biomass alone. Mean NDVI was found to be strongly correlated to mean total biomass ($R^2 = 0.969$) and mean LAI ($R^2 = 0.956$) when data are grouped into physiognomic categories (Figs 3a and 3b). Although the relationship between mean NDVI and mean IPAR for these categories appears to be strong, it is not significant at the 5% level (Fig. 3c). When the data are grouped into community types, mean NDVI was found to be significantly correlated to mean biomass ($R^2 = 0.856$) (Fig. 4). The curve that provides the best fit to these data is asymptotic, with the maximum NDVI value near 1.0. When data are ungrouped, the best fit between NDVI and biomass is again asymptotic (Fig. 5). This relationship is significant, but not strong ($R^2 = 0.267$). Mean field NDVI values and mean SPOT image NDVI values were found to be strongly correlated ($R^2 = 0.899$) (Fig. 6). However, field NDVI values were consistently about 40% higher than SPOT NDVI values.

The LAI and biomass images created from the SPOT NDVI image using the regression equations from the above analyses show trends in LAI and biomass across the landscape that are expected on the basis of geobotanical maps of the area (Walker and others 1989) (Fig. 7). Water tracks and south-facing slopes, both of which have dense

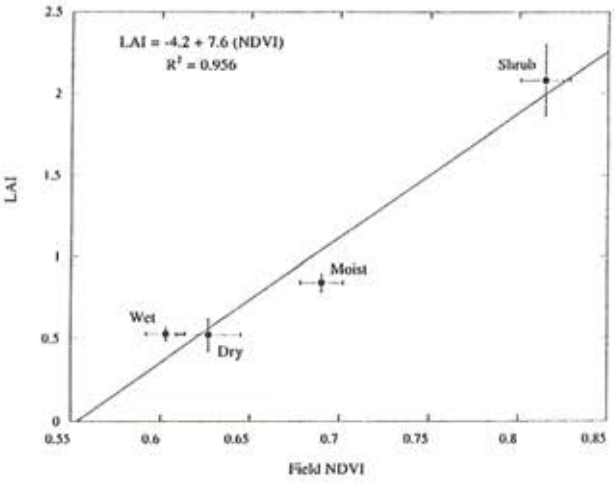


Fig. 3a. The relationships between NDVI and LAI when plots are grouped into physiognomic categories.

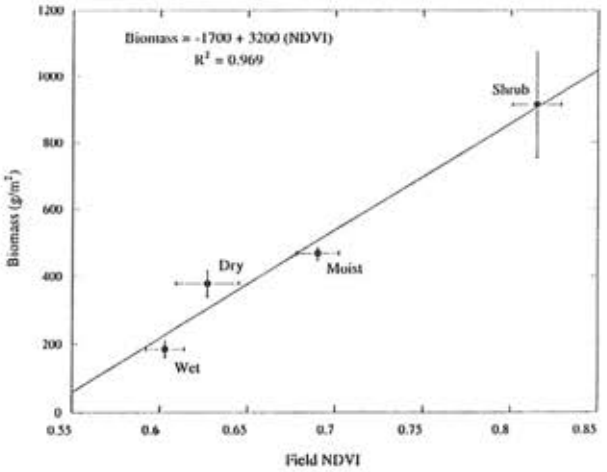


Fig. 3b. The relationships between NDVI and biomass when plots are grouped into physiognomic categories.

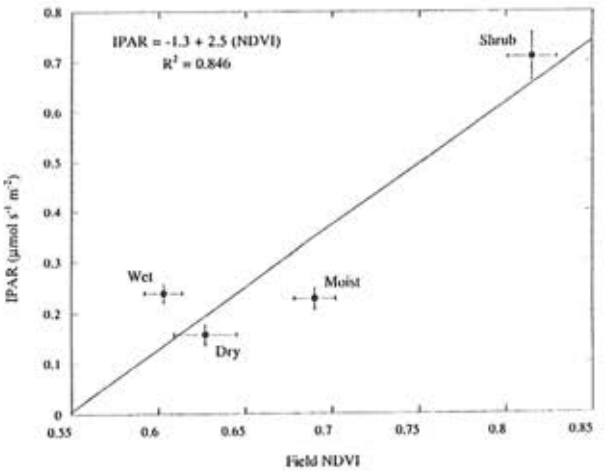


Fig. 3c. The relationships between NDVI and IPAR when plots are grouped into physiognomic categories.

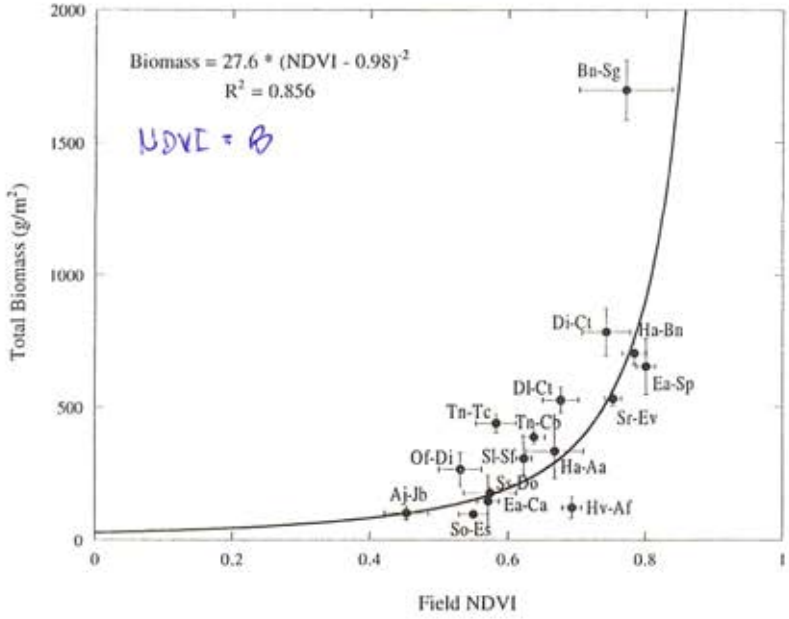


Fig. 4. The relationship between NDVI and biomass for the 180 plots grouped into categories by community type. Community type abbreviations are described in the caption of Figure 2.

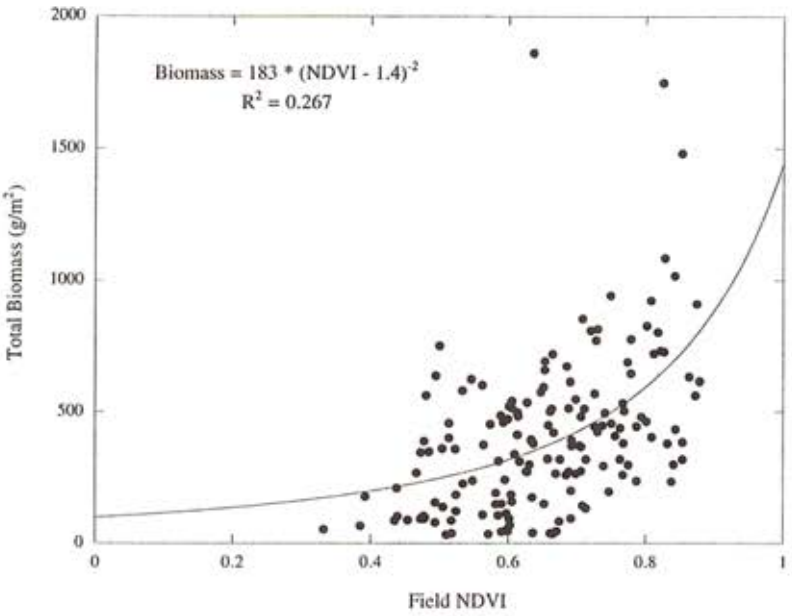


Fig. 5. The relationship between NDVI and biomass when replicate plots are ungrouped.

shrub vegetation, show LAI values greater than 3 and biomass values greater than 2000 g m$^{-2}$. Most barren hilltops and water bodies show LAI values of zero and biomass values less than 100 g m$^{-2}$. Wetlands generally show LAI values between zero and 1.0 and biomass values between 100 and 500 g m$^{-2}$. Upland interfluvial areas with tussock tundra vegetation have LAI values between 1.0 and 2.0 and biomass values between 500 and 1000 g m$^{-2}$. These values are consistent with values reported in the literature for the same area (Shaver and Chapin 1991). An image of IPAR was not calculated, because the relationship between NDVI and IPAR was not significant (Fig. 3c).

## Discussion

When the data for this study are grouped into the broad physiognomic categories, the curves that provide the best fit between NDVI and LAI or biomass are linear and quite strong (Figs 3a, 3b, 3c). This indicates that NDVI is linearly related to LAI and biomass in a general sense. However, as more detail is admitted into the analysis by breaking the data into more specific categories, individual vegetation types and plots deviate from this linear relationship. An asymptotic relationship is revealed, the strength of which is reduced with increasing detail (Figs 4 and 5). These results are consistent with recent discussions within the literature that assert that lowering resolution of models can increase predictability by averaging out chaotic behavior at the expense of losing detail about the phenomenon (Costanza and Maxwell 1994).

When the data are grouped into community types or left ungrouped, the curves that provide the best fit between NDVI and biomass are asymptotic (Figs 4 and 5). The asymptotic relationship between biomass and reflectance data for grass canopies has long been known (Tucker 1976). It is thought that as vegetation density increases, absorption approaches a maximum, beyond which any additional vegetation density would not contribute to the overall reflectance signature. An NDVI value near 1.0 would imply that the chlorophyll in the vegetation had absorbed all incident red light. This, therefore, is the theoretical maximum value for NDVI. The maximum NDVI value for the asymptotic curve relating mean NDVI to mean biomass for community types is indeed near 1.0.

The asymptotic relationship between mean NDVI and biomass for community types supports the results of Hansen (1991), which showed a strong exponential relationship between NDVI and biomass for data from many Arctic and sub-Arctic vegetation types. It is believed, however, that an asymptotic curve could be fitted to Hansen's data with good results. An asymptotic curve would make more physical sense than an exponential curve for reasons discussed above. These results in the present study, however, are quite different from those reported when only tussock tundra vegetation was considered (Auerbach

1992; Hope and others 1993). Both of those studies concluded that within tussock tundra, biomass is only one of the factors strongly influencing NDVI and that the other factors obfuscate any relationship that exists between NDVI and biomass. It appears that, within one vegetation type, NDVI and biomass may not be strongly related, whereas among many vegetation types the relationship can be quite strong. Therefore, NDVI may not be an appropriate means for estimating biomass when one is interested in detailed variations within one vegetation type. However, when one is interested in broad changes in biomass among very different vegetation types, NDVI may be an appropriate means for estimating biomass.

Some vegetation community types fall significantly outside the NDVI versus biomass curve (Fig. 4). The type *Betula nana-Salix glauca* has lower NDVI values than expected from the curve. This community type includes many shrubs, and it is likely that the wood in these shrubs contributes to high biomass measurements, but not to the chlorophyll absorption that is detected by NDVI. Several communities with abundant graminoid species (for example, *Tomenthypnum nitens-Tricophorum caespitosum* and *Tomenthypnum nitens-Carex bigelowii*) have lower values of NDVI than expected from the curve. This may be due to the large amounts of standing dead associated with graminoid vegetation, which does not contribute to chlorophyll absorption. Moreover, graminoid vegetation has a predominantly vertical leaf orientation, which results in lower NDVI values relative to those for canopies with horizontal leaf orientation (Sellers 1985).

All the analyses involving biomass were performed using both total above-ground biomass and photosynthetic biomass. In every case, the relationships between biomass and NDVI are considerably stronger when total above-ground biomass is used. This is counter-intuitive, because it was expected that the presence of non-photosynthetic material should weaken the absorption in red wavelengths. However, Sellers (1985)

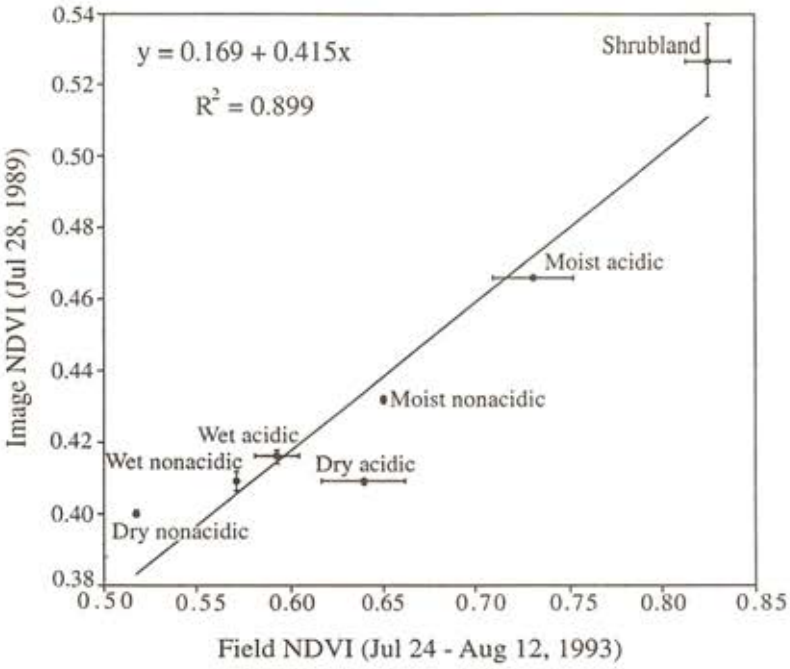


Fig. 6. The relationship between mean field NDVI and mean SPOT image NDVI for vegetation community groups (see Fig. 2).

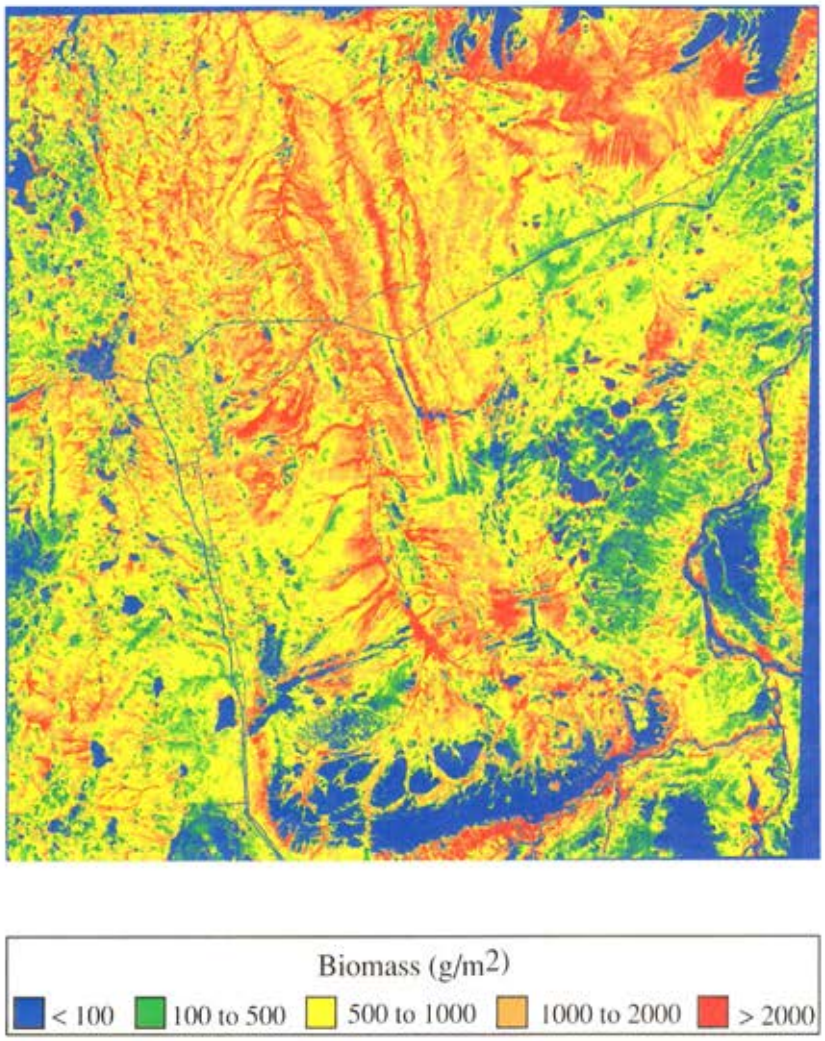

suggested that the relationship between LAI and NDVI should be weaker when non-photosynthetic material is present than when it is not, even if only photosynthetic material is included in the calculation of LAI. Perhaps this effect also causes a weaker relationship between LAI and NDVI when only photosynthetic material is considered than when all material is considered. In addition, perhaps a similar effect causes the stronger relationships noted here between total biomass and NDVI than between photosynthetic biomass and NDVI.

Many different factors probably contribute to the higher NDVI values from field spectra than from SPOT spectra (Fig. 6). These include low sun angle in combination with relatively high view angle of the SPOT sensor. Because of this lighting geometry, the SPOT sensor receives backscattered light, while the field sensor receives forward-scattered light. Forward-scattered light travels through more vegetation, thus saturating the chlorophyll absorption features, resulting in higher NDVI values. In addition, the SPOT sensor sees less shadow due to the low angle between incident light and the light reflected toward the sensor. Shadows decrease the reflectance at all wavelengths, resulting in higher NDVI values. More atmosphere is also present between the SPOT sensor and the vegetation than between the field sensor and the vegetation. Although a dark object subtraction was applied to the SPOT image to correct for atmospheric effects, this correction is only an approximation. The field sensor is corrected for atmospheric effects immediately prior to data collection, thereby minimizing effects of atmosphere. This is not possible for the satellite-born SPOT sensor. Atmospheric interference would result in higher red reflectances and therefore lower NDVI values. Finally, the SPOT sensor integrates reflectance data over the 20 x 20 m area of its instantaneous field of view. The field sensor, on the other hand, integrates reflectance data from a circular field of view with a radius of approximately 10 cm. The areas chosen to be measured with the field sensor did not include bare patches, water, or rocks. The SPOT sensor mixes signals from all materials within its field of view, including bare patches, water, and rocks, which undoubtedly lower the NDVI values reported for each vegetation type.

The biomass and LAI images calculated from the SPOT NDVI image using the regression equations in Figure 3 have values consistent with those previously reported for the region (Shaver and Chapin 1991) (Fig. 7), except for shrublands where the values are slightly higher in the images. A possible explanation for this discrepancy is that Shaver and Chapin sampled only one shrub site, and this site may have had lower biomass and LAI than many other shrublands in the area.

Fig. 7. Images of biomass (opposite) and LAI (below), generated from a SPOT NDVI image using the relationships between biomass, LAI, and NDVI observed in this study.

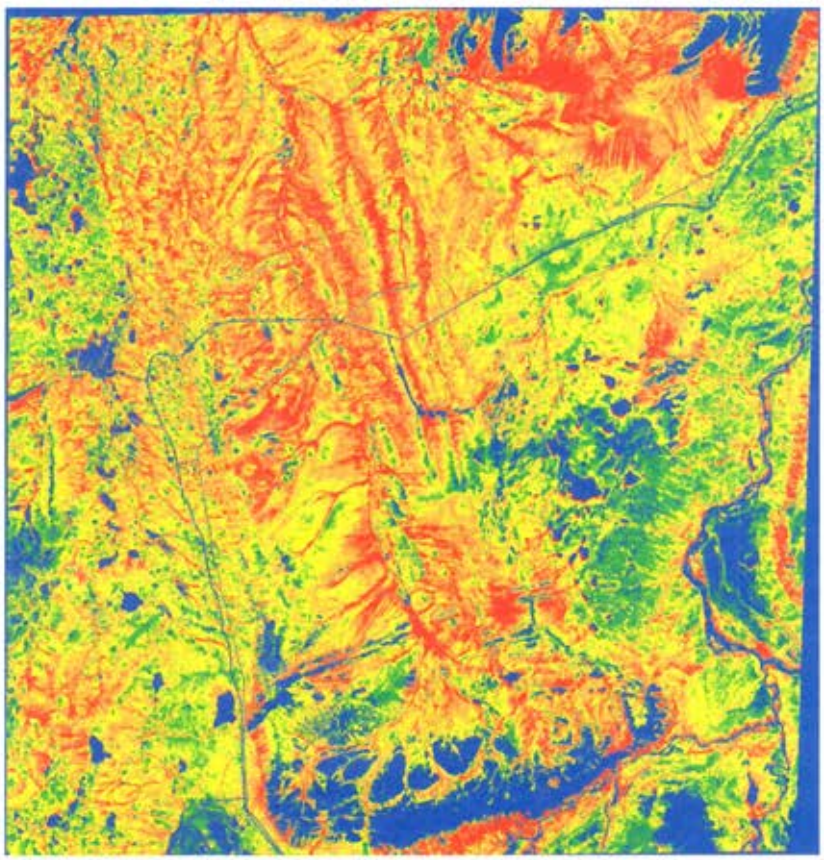

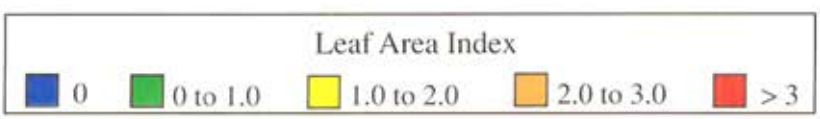


## Conclusions

When the data from this study are grouped into broad physiognomic categories, the relationships between NDVI and biomass or LAI are linear and strong. The relationship between NDVI and IPAR is not significant. When data from this study are grouped into community types the relationships between NDVI and biomass are strong and asymptotic, with maximum NDVI values near 1.0. When the data from this study are left ungrouped, the relationship between NDVI and biomass is asymptotic, but not strong.

Reducing the detail of these analyses increases the predictability by averaging out chaotic behavior at the expense of losing detail about the relationship.

Within one vegetation type, NDVI and biomass may not be

strongly related, whereas among many vegetation types the relationship can be strong.

Low sun angle, high view angle of the SPOT sensor, atmospheric effects, and spatial resolution all contribute to lower NDVI values for community types from the SPOT image than from the field sensor.

The LAI and biomass images calculated from the SPOT NDVI image using the regression equations discussed above provide realistic representations of the spatial variation and magnitudes of LAI and biomass in this area.

## Acknowledgements

The authors would like to thank David Schimel for valuable discussions that generated many of the ideas included in this manuscript. We would also like to thank Carol Wessman for providing the LI-COR plant canopy analyzer. This research was funded by NSF/DPP grant 9214959.

## References

Asrar, G., E.T. Kanemasu, R.D. Jackson, and P.J. Pinter. 1985. Estimation of total above-ground phytomass production using remotely sensed data. *Remote Sensing of Environment* 17: 211–220.

Auerbach, N.A. 1992. Effects of road and dust disturbance in minerotrophic and acidic tundra ecosystems, northern Alaska. Unpublished MS thesis, University of Colorado.

Baret, G. and G. Guyot. 1991. Potentials and limits of vegetation indices for LAI and APAR assessment. *Remote Sensing of Environment* 35: 161–173.

Biscoe, P.V., J.N. Gallagher, E.J. Littleton, J.L. Monteith, and R.K. Scott. 1975. Barley and its environment, IV. Sources of assimilate for the grain. *Journal of Applied Ecology* 12: 295–318.

Box, E.O., B.N. Holben, and V. Kalb. 1989. Accuracy of the AVHRR vegetation index as a predictor of biomass, primary productivity and net $CO_2$ flux. *Vegetation* 80: 71–89.

Colwell, J.E. 1973. Bidirectional spectral reflectance of grass canopies for determination of above ground standing biomass. Unpublished PhD thesis, University of Michigan.

Colwell, J.E. 1974. Vegetation canopy reflectance. *Remote Sensing of Environment* 3: 175–183.

Costanza, R., and T. Maxwell. 1994. Resolution and predictability: an approach to the scaling problem. *Landscape Ecology* 9 (1): 47–57.

Gallo, K.P., and C.S.T. Daughtry. 1987. Differences in vegetation indices for simulated Landsat-5 MSS and TM, NOAA-9 AVHRR, and SPOT-1 sensor systems. *Remote Sensing of Environment* 23: 439–452.

Hansen, B.U. 1991. Monitoring natural vegetation in southern Greenland using NOAA AVHRR and field measurements. *Arctic* 44 (1): 94–101.

Hatfield, J.L., G. Asrar, and E.T. Kanemasu. 1984. Intercepted photosynthetically active radiation estimated by spectral reflectance. *Remote Sensing of Environment* 14: 65–75.

Hodges, T., and E.T. Kanemasu. 1977. Modeling daily dry matter production of winter wheat. *Agronomy Journal* 69: 974–978.

Hope, A.S., J.S. Kimball, and D.A. Stow. 1993. The relationship between tussock tundra spectral reflectance properties and biomass and vegetation composition. *International Journal of Remote Sensing* 14 (10): 1861–1874.

Jordan, C.F. 1969. Derivation of leaf-area index from quality of light on the forest floor. *Ecology* 50: 663–666.

Perry, C.R., and L.F. Lautenschlager. 1984. Functional equivalence of spectral vegetation indices. *Remote Sensing of Environment* 14: 169–182.

Prince, S.D. 1991. Satellite remote sensing of primary production: comparison of results for Sahelian grasslands 1981–1988. *International Journal of Remote Sensing* 12 (6): 1301–1311.

Rouse, J.W., R.H. Haas, J.A. Schell, and D.W. Deering. 1973. Monitoring vegetation systems in the great plains with ERTS. In: *Third ERTS Symposium*. Greenbelt, MD: NASA (SP-351) 1: 309–317.

Rouse, J.W., R.H. Haas, J.A. Schell, D.W. Deering, and J.C. Harlan. 1974. Monitoring the vernal advancement and retrogradation (greenwave effect) of natural vegetation. Greenbelt, MD: NASA/GSFC (Type III Final Report).

Sellers, P.J. 1985. Canopy reflectance, photosynthesis and transpiration. *International Journal of Remote Sensing* 6 (8): 1335–1372.

Sellers, P.J. 1987. Canopy reflectance, photosynthesis and transpiration. II: The role of biophysics in the linearity of their interdependence. *Remote Sensing of Environment* 21: 143–183.

Sellers, P.J. 1992. Canopy reflectance, photosynthesis, and transpiration. III: A reanalysis using improved leaf models and a new canopy integration scheme. *Remote Sensing of Environment* 42: 187–216.

Shaver, G., and F.S. Chapin III. 1991. Production: biomass relationships and element cycling in contrasting Arctic vegetation types. *Ecological Monographs* 61 (1): 1–31.

Steven, M.D., P.V. Biscoe, K.W. Jaggard. 1983. Estimation of sugarbeet productivity from reflection in the red and infrared spectral bands. *International Journal of Remote Sensing* 4: 325–334.

Stow, D.A., A.S. Hope, and T.H. George. 1993. Reflectance characteristics of Arctic tundra vegetation from airborne radiometry. *International Journal of Remote Sensing* 14 (6): 1239–1244.

Tucker, C.J. 1976. Asymptotic nature of grass canopy spectral reflectance. *Applied Optics* 16 (5): 1151–1156.

Tucker, C.J., and P.J. Sellers. 1986. Satellite remote sensing of primary production. *International Journal of Remote Sensing* 7 (11): 1395–1416.

Walker, D.A., N.A. Auerbach, and M.M. Shippert. 1995. NDVI, biomass, and landscape evolution of glaciated terrain in northern Alaska. *Polar Record* 31 (177): 169–178.

Walker, D.A., E.F. Binnian, B.M. Evans, N.D. Lederer, E. Nordstrand, and P.J. Webber. 1989. Terrain, vegetation and landscape evolution of the DOE R4D research site, Brooks Range foothills, Alaska. *Holarctic Ecology* 12: 238–261.

Walker, D.A., and M.D. Walker. 1991. History and pattern of disturbance in Alaskan Arctic terrestrial ecosystems: a hierarchical approach to analyzing landscape change. *Journal of Applied Ecology* 28: 244–276.

Wiegand, C.L., A.J. Richardson, and E.T. Kanemasu. 1979. Leaf area index estimates for wheat from Landsat and their implications for evapotranspiration and crop modeling. *Agronomy Journal* 71: 336–342.

*The accuracy of references in the text and in this list is the responsibility of the authors, to whom queries should be addressed.*